Mouse bone marrow mesenchymal stem cells with distinct p53 statuses display differential characteristics

BO WANG[1*], LINGXIA WANG[2*], JIAHUI MAO[3], HUIYAN WEN[2], LONGJIANG XU[4], YANG REN[1], HONG DU[2] and HUAN YANG[2]

Departments of [1]Oncology and [2]Clinical Laboratory, The Second Affiliated Hospital of Soochow University, Suzhou, Jiangsu 215004; [3]Department of Central Laboratory, The Affiliated Hospital of Jiangsu University, Zhenjiang, Jiangsu 212013; [4]Department of Pathology, The Second Affiliated Hospital of Soochow University, Suzhou, Jiangsu 215004, P.R. China

Received May 20, 2019; Accepted November 26, 2019

DOI: 10.3892/mmr.2020.11025

Abstract. Mesenchymal stem cells (MSCs) affect diverse aspects of tumor progression, such as angiogenesis, tumor growth and metastasis. Bone marrow MSCs (BM-MSCs) are fibroblast-like cells with multipotent differentiation ability, that localize to areas of tissue damage, including wounds and solid tumors. The tumor suppressor gene, p53, is functionally involved in cell cycle control, apoptosis and genomic stability, and is mutated and inactivated in most human cancers. The present study aimed to investigate the role of p53 in the biology of BM-MSCs. In the present study, p53 wild-type ($p53^{+/+}$), knockdown ($p53^{+/-}$) and knockout ($p53^{-/-}$) mouse BM-MSCs (mBM-MSCs) were observed to be similar in appearance and in the expression of cell surface biomarkers, but expressed differential p53 protein levels. The $p53^{+/-}$ and $p53^{-/-}$ mBM-MSCs demonstrated an increased proliferation rate compared with mBM-MSCs derived from $p53^{+/+}$ mice. mBM-MSCs from all three groups, representing distinct p53 statuses, were unable to form tumors over a 3-month period *in vivo*. The adipogenic and osteogenic differentiation of mBM-MSCs was increased in the absence of p53. The colony formation and migratory abilities of $p53^{+/-}$ and $p53^{-/-}$ mBM-MSCs were markedly enhanced, and the expression levels of stem cell-associated proteins were significantly increased compared with $p53^{+/+}$. The expression levels of microRNA (miR)-3152 and miR-337 were significantly increased in $p53^{+/-}$ and $p53^{-/-}$ mBM-MSCs, whereas the expression levels of miR-221, miR-155, miR-1288 and miR-4669 were significantly decreased. The expression levels of tumor necrosis factor-α and interferon-γ-inducible protein-10 were significantly upregulated in the supernatant of $p53^{+/-}$ and $p53^{-/-}$ mBM-MSCs. Ubiquitin protein ligase E3 component n-recognin 2, RING-finger protein 31 and matrix metalloproteinase 19 were highly expressed in $p53^{+/-}$ and $p53^{-/-}$ mBM-MSCs. The results of the present study indicated that p53 may serve an important role in the biology of mBM-MSCs, and may provide novel insights into the role of cells with different p53 statuses in cancer progression.

Correspondence to: Professor Huan Yang or Professor Hong Du, Department of Clinical Laboratory, The Second Affiliated Hospital of Soochow University, 1055 Sanxiang Road, Suzhou, Jiangsu 215004, P.R. China
E-mail: soochowyh@163.com
E-mail: hong_du@126.com

*Contributed equally

Key words: p53, mouse bone marrow mesenchymal stem cells

Introduction

Adult mesenchymal stem cells (MSCs) are fibroblast-like, multipotent cells that can be isolated from bone marrow (BM), adipose tissue, umbilical cord, skeletal muscle, liver and tumoral tissues (1-3). MSCs display unique characteristics that enable them to develop into several different cell types, including osteoblasts, adipocytes, chondrocytes and hematopoiesis-supportive stroma (4); they can be mobilized from BM, and other tissues, to sites of inflammation, such as areas of injury and tumors (5-8), respond to the local microenvironment, and exert immunosuppressive and anti-inflammatory activities (9,10). Previous studies have reported that MSCs can promote the growth, metastasis and invasion of cancers (11-13); for example, Zhu *et al* (14) demonstrated that the inhibition of microRNA (miR)-155-5p promoted the transition of BM-MSCs into gastric cancer-MSCs through the activation of the NF-κB p65-signaling pathway. MSCs also reportedly induce the expression of discoidin domain-containing receptor 2 to mediate the growth and metastasis of breast cancer (8). MSC senescence influences the growth, metastasis and angiogenesis of colon cancer by secreting galectin-3 (15), and MSCs are reported to represent promising potential for their use in cancer therapy; with Zhang *et al* (16) demonstrating that MSCs have potential beneficial effects for breast cancer therapy through the targeting of fibronectin 1, CD44 and nerve growth factor.

p53 is a prominent transcription factor and tumor suppressor gene that regulates the homeostasis of cells (17), as well as several cellular processes, such as cell cycle control

and growth, differentiation and DNA repair; therefore, p53 is often referred to as the guardian of the genome (18). A mutation or loss of p53 expression occurs in ~50% of human cancers (19,20), and p53 mutations can lead to genome instability, functional alterations in cell proliferation, migration, differentiation and the cell cycle, and the aberrant transformation of MSCs. For example, the absence of p53 can increase the osteogenic differentiation of BM-MSCs (21-23), and the inactivation of p53 skews MSCs towards an osteogenic fate and impairs hematopoiesis-supporting activity (24). p53 abnormality is correlated with the transformation of MSCs, which promotes mesodermal tumor formation (18,25,26).

The differential characteristics of mouse (m)BM-MSCs exhibiting distinct p53 statuses has not been thoroughly investigated. In the present study, the characteristics of mBM-MSCs obtained from p53 wild-type ($p53^{+/+}$), p53 knockdown ($p53^{+/-}$) and p53 knockout ($p53^{-/-}$) mice were analyzed to investigate their abilities to grow, differentiate and target stemness-related proteins, in addition to their ability to target miRNA and protein expression, as well as inflammatory cytokine secretion, to provide novel evidence for the role of stromal p53.

Materials and methods

Animal studies and the isolation and culture of mBM-MSCs. All experimental procedures involving animals were conducted in accordance with the Guide for the Care and Use of Laboratory Animals and were approved by the Animal Use Ethics Committee of Jiangsu University (Zhenjiang, China). A total of 18 C57BL/6 mice (sex, male; weight, 15-20 g; age, 6-8 weeks; n=6/group) with a $p53^{+/+}$, $p53^{+/-}$ or $p53^{-/-}$ genotype were obtained from Nanjing Medical University (Nanjing, China), and were housed under standard conditions at 20-26˚C and 40-70% humidity, in a 12-h light/dark cycle with free access to food and water. Mice were euthanized by CO_2 inhalation; mice were placed in an enclosed box and CO_2 was released at a flow rate of 2.5 l/min, with a displacement rate of 28% volume/min. Death was ensured following confirmation that the mice exhibited no breathing, pupil dilation and no heartbeat. The BM was collected from mice by flushing the femurs. Cells from the BM were cultured in DMEM with low glucose (Invitrogen; Thermo Fisher Scientific, Inc.), supplemented with 15% FBS (Invitrogen; Thermo Fisher Scientific, Inc.) and 50 U/ml penicillin/streptomycin (Gibco; Thermo Fisher Scientific, Inc.), and maintained in a humidified atmosphere at 37˚C with 5% CO_2 for 4 days to facilitate attachment. Non-adherent cells were removed after 4 days incubation by changing the culture medium. Cells were trypsinized with 0.25% trypsin/0.1% EDTA (Sigma-Aldrich, Merck KGaA) and re-plated at $8x10^3$ cells/cm^2 (approximately 1:3), and the medium was changed every 3 days. Homogeneous fibroblast-like cell populations appeared after five passages, and mBM-MSCs obtained at passage five were used for subsequent experimentation.

Morphology detection. mBM-MSCs were cultured in DMEM with low glucose (Invitrogen; Thermo Fisher Scientific, Inc.), supplemented with 15% FBS (Invitrogen; Thermo Fisher Scientific, Inc.). Cells were trypsinized with 0.25% trypsin/0.1% EDTA (Sigma-Aldrich; Merck KGaA) and re-plated at $8x10^3$ cells/cm^2 for 12 h at 37˚C. Cells were subsequently visualized using an Olympus CKX41 inverted phase contrast light microscope (magnification, x20).

Flow cytometry. mBM-MSCs were trypsinized with 0.25% trypsin/0.1% EDTA and washed twice with 10.2 g/l PBS (pH=7.2). Cells were subsequently incubated on ice with the following monoclonal antibodies (1:250): FITC-conjugated CD29 (cat. no. 561796; BD Pharminogen; BD Biosciences), FITC-conjugated CD34 (cat. no. 560238; BD Pharminogen; BD Biosciences), FITC-conjugated CD90 (cat. no. 561973; BD Pharminogen; BD Biosciences), phycoerythrin (PE)-conjugated CD44 (cat. no. 553134; BD Pharminogen; BD Biosciences), PE-conjugated CD45 (cat. 553081; BD Pharminogen; BD Biosciences) or PE-conjugated CD11b (cat. no 12-0112-82; eBioscience; Thermo Fisher Scientific, Inc.). PE- and FITC-conjugated IgM and IgG were used as controls. Labeled cells were analyzed by flow cytometry using a BD FACSCaliburä flow cytometer (BD Biosciences) and FlowJo version 10 software (Tree Star, Inc.).

Growth curves. $p53^{+/+}$, $p53^{+/-}$ and $p53^{-/-}$ mBM-MSCs were seeded in 24-well plates ($5x10^3$ cells/well) during the logarithmic growth phase, and the number of cells/well was counted on 12 consecutive days manually. Briefly, the cells in the three duplicated wells were digested and the number of cells were counted using an abalone counting board.

Cell cycle analysis. To determine DNA synthesis, the cells were trypsinized and harvested by centrifugation (25˚C; 92 x g; 5 min). The pellets were resuspended in 0.1% PBS and subsequently fixed with 75% ethanol at -20˚C for 12 h, and then permeabilized with 0.1% Triton X-100 at room temperature for 20 min. Following treatment with RNase at 37˚C for 30 min, the cells were incubated with propidium iodide (50 μg/ml) at 25˚C for 15 min. Cells were analyzed by flow cytometry using a BD FACSCalibur™ flow cytometer (BD Biosciences). The percentage of cells in the G1, S and G2 phases were quantified using BD CellQuestä version 5.1 software (BD Biosciences).

Tumor formation assay. For the tumor formation assay, BALB/c nu/nu mice (age, 4 weeks; sex, male; weight, 15-20 g; n=6/group) obtained from The Shanghai Animal Laboratory Center of the Chinese Academy of Sciences, were injected subcutaneously under the armpit with $1x10^6$ and $5x10^6$ $p53^{+/+}$, $p53^{+/-}$ or $p53^{-/-}$ mBM-MSCs (passage no. 9, 11, 13 or 15) suspended in 200 μl 0.1% PBS, and the incidence of tumor formation was observed for 3 months. Mice were euthanized as previously described above at 3 months prior to measuring the tumor size.

Hematoxylin & eosin staining. Tumor sections were fixed in formalin for 24 h at room temperature and embedded in paraffin. Paraffin-embedded tissues were cut into 4-6-μm thick sections. The tissue sections were subsequently deparaffinized in xylene for 12 h at 75˚C, rehydrated using a descending ethanol series (100, 95, 85 and 75% for 2 min each) and then boiled for 30 min in 10 mM citrate buffer (pH 6.0) for antigen retrieval. Endogenous peroxidase activity was inhibited by exposing the sections to 3% hydrogen peroxide for 10 min at room temperature. Sections were stained with 0.2% hematoxylin for 5 min at room temperature and then 0.5% eosin

for 1-3 min at room temperature. Stained cells were visualized using an Olympus CKX41 inverted phase contrast light microscope (magnification, x100; Olympus Corporation).

Adipogenic and osteogenic differentiation in vitro. $p53^{+/+}$, $p53^{+/-}$ and $p53^{-/-}$ mBM-MSCs were seeded at $5x10^3$ cells/cm^2 in 35-mm plates and cultured in L-DMEM (Invitrogen; Thermo Fisher Scientific, Inc.) with 15% FBS (Invitrogen; Thermo Fisher Scientific, Inc.), and either adipogenic [1 μM dexamethasone and 10 μg/ml insulin (Sigma-Aldrich, Merck KGaA)] or osteogenic [0.1 μM dexamethasone, 10 μM β-glycerophosphate, 50 μg/l ascorbic acid, and 4 μg/ml basic fibroblast growth factor (Sigma-Aldrich, Merck KGaA)] supplements for a total induction period of 1-2 weeks; with the medium being changed three times/week. Following induction, intracellular lipid accumulation was visualized using Oil Red O staining. Briefly, cells were fixed with 10% neutral formaldehyde for 30 min at room temperature and were subsequently incubated with 0.5% Oil Red O solution for 10 min at room temperature. Osteogenic differentiation was assessed by examining alkaline phosphatase activity through alkaline phosphatase staining. Briefly, the cells were fixed in 10% formalin methanol solution for 10 min at 0.5˚C and subsequently washed in distilled water. Cells were stained with a solution containing 35 mg α-phosphate naphthol sodium, 35 mg Fast Garnet and 35 ml 0.05 M acrylamide for 5-10 min at room temperature. The cells were subsequently washed with tap water for 10 min and the cytoplasm of the cells could be viewed as light red granules. Cells cultured in basic medium were stained with the two staining reagents, as described above, to serve as the negative controls. Stained cells were visualized using an Olympus CKX41 inverted phase contrast light microscope (magnification, x100; Olympus Corporation).

Colony formation assay. $p53^{+/+}$, $p53^{+/-}$ and $p53^{-/-}$ mBM-MSCs were harvested, seeded at $1x10^3$ cells/well in 35-mm plates, and incubated in a humidified atmosphere at 37˚C and 5% CO_2 for 14 days; with the L-DMEM, supplemented with 15% FBS (Invitrogen; Thermo Fisher Scientific, Inc.) being replaced every 3 days. Following incubation, colonies were subsequently fixed with 4% paraformaldehyde for 20 min at room temperature prior to being stained with 0.5% crystal violet at room temperature for 20 min. Stained colonies of 0.3-1.0 mm were counted using a Vernier Caliper and the formation of colonies was semi-quantified using ImageJ version 1.8.0 software (National Institutes of Health).

Transwell migration assay. A total of $1x10^5$ $p53^{+/+}$, $p53^{+/-}$ and $p53^{-/-}$ mBM-MSCs/well were plated in the upper chambers of Transwell plates (Corning Inc.) with serum-free DMEM, and DMEM, supplemented with 15% FBS was plated in the lower chambers. Following incubation for 12 h at 37˚C, the cells remaining on the upper surface of the membrane were removed with a cotton swab. The cells that migrated through the 8-mm pores and adhered to the lower surface of the membrane were fixed with 4% paraformaldehyde at room temperature for 20 min, and subsequently stained with 0.5% crystal violet at room temperature for 20 min. Stained cells were visualized using an Olympus CKX41 inverted phase contrast light microscope (magnification, x20; Olympus Corporation).

Reverse transcription-quantitative PCR (RT-qPCR). Total RNA was extracted from $p53^{+/+}$, $p53^{+/-}$ and $p53^{-/-}$ mBM-MSCs using TRIzol® reagent (Invitrogen; Thermo Fisher Scientific, Inc.), according to the manufacturer's protocol. Total RNA was reverse transcribed into cDNA using the miScriptIIRT kit (cat. no. 218161; Qiagen China Co., Ltd.), according to the manufacturer's protocol. The following RT temperature protocol was used: 37˚C for 1 h and 95˚C for 5 min. qPCR was subsequently performed using the miScript SYBR Green PCR kit (cat. no. 218073; Qiagen China Co., Ltd.), according to the manufacturer's protocol, and the CFX96 Touch Real-Time PCR detection system (Bio-Rad Laboratories, Inc.). The primer pairs used for the qPCR were obtained from Qiagen (cat. no. 218073; Qiagen China Co., Ltd.). The following thermocycling conditions were used for the qPCR: Initial denaturation at 95˚C for 10 min; and 40 cycles of 95˚C for 10 sec, 55˚C for 30 sec and 72˚C for 32 sec. miRNA expression levels were quantified using the $2^{-\Delta\Delta Cq}$ method (27) and normalized to the internal reference gene U6.

Western blotting. Total protein was extracted from $p53^{+/+}$, $p53^{+/-}$ and $p53^{-/-}$ mBM-MSCs using RIPA buffer supplemented with protease inhibitors (Santa Cruz Biotechnology, Inc.). Total protein concentration was quantified using a BCA assay kit (Thermo Fisher Scientific, Inc.) and 40 μg protein/lane was separated by 10% SDS-PAGE. Following electrophoresis, the separated proteins were subsequently transferred onto a PVDF membrane and blocked in 5% (w/v) non-fat milk for 1 h at room temperature. The membranes were incubated with the following primary antibodies: Anti-GAPDH (1:1,000; cat. no. KC-5G5; Kangchen BioTech Co., Ltd.), anti-p53 (1:1,000; cat. no. abs130596; Absin Bioscience, Inc.), anti-Sal-like protein 4 (SALL4); (1:500; cat. no. ab29112; Abcam), anti-protein lin-28 homolog B (LIN28B; 1:500; cat. no. 21626; Signalway Antibody LLC), anti-Sox2 (1:500; cat. no. ab5603; EMD Millipore), anti-octamer-binding protein 4 (Oct4; 1:400; cat. no. 21424; Signalway Antibody LLC), anti-c-Myc (1:200; cat. no. 10057-1-AP; ProteinTech Group, Inc.), anti-ubiquitin protein ligase E3 component n-recognin 2 (UBR2; 1:500; cat. no. BS60150; Bioworld Technology, Inc.), anti-matrix metalloproteinase 19 (MMP19; 1:500; cat. no. BS1235; Bioworld Technology, Inc.) and anti-RING-finger protein 31 (RNF31; 1:500; cat. no ab46322; Abcam). Following the primary incubation, membranes were incubated for 1 h at room temperature with horseradish peroxidase-conjugated secondary antibodies: Goat anti-rabbit IgG (1:2,000; cat. no. CW0103; CoWin Biosciences) and goat anti-mouse IgG (1:2,000; cat. no. CW0102; CoWin Biosciences). Protein bands were visualized using the Immobilon Western Chemiluminescent HRP substrate (EMD Millipore). GAPDH was used as the loading control. Expression levels were quantified using ImageJ version 1.8.0 software (National Institutes of Health).

Luminex assay. Supernatants from $p53^{+/+}$, $p53^{+/-}$ and $p53^{-/-}$ mBM-MSCs were collected by centrifugation (500 x g; 10 min; 25˚C) to remove cellular debris following 6-8 h of cell culture. The MILLIPLEX MAP Mouse Cytokine/Chemokine Magnetic Bead Panel kit (cat. no. MCYTOMAG-70K-12; Sigma-Aldrich; Merck KGaA) was used to assess cytokine levels of tumor necrosis factor (TNF)-α and interferon-γ-inducible protein

(IP)-10 in the supernatants, according to the manufacturer's protocol. The final detection and analysis were performed using the Luminex 200™ system (Merck KGaA).

Statistical analysis. All data are expressed as the mean ± SD from ≥3 independent experimental repeats. The statistical differences between groups were determined using an one-way ANOVA, followed by Tukey's range test using GraphPad Prism version 5 (GraphPad Software, Inc.). $P<0.05$ was considered to indicate a statistically significant difference.

Results

Morphology of mBM-MSCs and p53 protein expression. Following the initial 8-14 days (passage 5) in culture, mBM-MSCs adhered to a plastic surface and presented as a mixture of fibroblastic and hematopoietic cell types, as determined by the expression of surface markers (Figs. S1 and S2). Following 20 days from initial plating, the cells demonstrated a long, spindle-shaped fibroblast phenotype, began to form colonies and become confluent. After being re-plated for 20 days, the fibroblast-like cells appeared polygonal or spindly, with a long process and an orderly pattern at confluence (Fig. 1A). The $p53^{+/+}$, $p53^{+/-}$ and $p53^{-/-}$ mBM-MSCs were observed to share similar phenotypes on the basis of typical morphology. $p53^{+/+}$ mBM-MSCs expressed the highest levels of p53 protein, whilst $p53^{+/-}$ mBM-MSCs displayed intermediate expression levels of p53 protein and $p53^{-/-}$ mBM-MSCs expressed very little levels of p53 protein (Fig. 1B).

Surface antigens. Following five cell passages, $p53^{+/+}$, $p53^{+/-}$ and $p53^{-/-}$ mBM-MSCs were characterized by determining the expression of stem cell markers, CD29 (98.68, 99.74 and 99.72%, respectively), CD44 (99.50, 99.06 and 99.43%, respectively) and CD90 (98.55, 97.43 and 98.71%, respectively), hemocyte markers, CD34 (3.85, 2.67 and 4.99%, respectively) and CD45 (4.85, 0.42 and 0.95%, respectively), and the macrophage marker, CD11b (2.41, 2.72 and 2.58%, respectively; Figs. 2, S1 and S2). The three types of mBM-MSCs were all positive for CD29, CD44 and CD90, but were negative for CD45, CD34, and CD11b.

Cell cycle analysis of mBM-MSCs. $p53^{+/+}$ mBM-MSCs demonstrated slow growth rate throughout the 12-day culture (Fig. 3A); however, 3 days post-seeding, $p53^{-/-}$ mBM-MSCs began to expand rapidly and move into the logarithmic phase of growth. At day 9, cell counts reached their highest levels in $p53^{-/-}$ mBM-MSCs, before subsequently entering the plateau phase. At 3 days post-seeding, the number of $p53^{-/-}$ mBM-MSCs was ~2 times that of $p53^{+/+}$ mBM-MSCs. From day 6, the number of $p53^{+/-}$ mBM-MSCs was greater than that of $p53^{+/+}$ mBM-MSCs. $p53^{-/-}$ mBM-MSCs were observed to grow faster than $p53^{+/-}$ mBM-MSCs from day 3 until day 12 (Fig. 3A). Cell cycle analysis indicated that the S phase rate of $p53^{-/-}$ and $p53^{+/-}$ mBM-MSCs was significantly higher compared with $p53^{+/+}$ mBM-MSCs (Fig. 3B), and $p53^{-/-}$ mBM-MSCs demonstrated an increased S phase rate compared with $p53^{+/-}$ mBM-MSCs (Fig. 3B).

mBM-MSCs are unable to form spontaneous tumors in mice regardless of p53 status. To study the ability of $p53^{+/+}$, $p53^{+/-}$ and $p53^{-/-}$ mBM-MSCs to induce tumor formation, different numbers of cells from different passages were subcutaneously injected into BALB/c nu/nu mice. Three months after injection, no tumors were observed to have formed in mice from any group, regardless of the number of cells injected or the cell passage number used. Thus, $p53^{+/+}$, $p53^{+/-}$ and $p53^{-/-}$ mBM-MSCs were unable to form spontaneous transformation in mice within a three-month period.

Differentiation of mBM-MSCs into adipocytes and osteocytes. $p53^{+/-}$ and $p53^{-/-}$ mBM-MSCs induced with adipogenic medium for 2 weeks were observed to contain a significant number of Oil Red O-positive lipid droplets compared with $p53^{+/+}$ mBM-MSCs (Fig. 4A); in addition, $p53^{-/-}$ mBM-MSCs exhibited significantly more positive cells compared with $p53^{+/-}$ mBM-MSCs. Following osteogenic supplementation, $p53^{-/-}$ mBM-MSCs had significantly more alkaline phosphatase-positive cells compared with $p53^{+/-}$ mBM-MSCs, and both demonstrated significantly enhanced osteogenic differentiation levels compared with $p53^{+/+}$ mBM-MSCs (Fig. 4B). Thus, overall, the $p53^{+/+}$ mBM-MSCs displayed very little adipogenic or osteogenic differentiation.

Colony formation and migratory ability of mBM-MSCs. Colony formation assay analysis demonstrated that $p53^{+/-}$ and $p53^{-/-}$ mBM-MSCs formed significantly more colonies compared with $p53^{+/+}$ mBM-MSCs (Fig. 5A); in addition, $p53^{-/-}$ mBM-MSCs were observed to form significantly more colonies compared with $p53^{+/-}$ mBM-MSCs. The role of p53 in regulating mBM-MSC motility was determined using the Transwell migration assay. Compared with $p53^{+/+}$ mBM-MSCs, the migratory rate of $p53^{+/-}$ and $p53^{-/-}$ mBM-MSCs was significantly increased (Fig. 5B); however, there was no significant difference between the migration rate of $p53^{+/-}$ and $p53^{-/-}$ mBM-MSCs (Fig. 5B).

Expression of stem cell-associated proteins in mBM-MSCs. Western blot analysis revealed that stem cell-related proteins LIN28B, Sox2, c-Myc, SALL4 and Oct4 were expressed at significantly higher expression levels in $p53^{+/-}$ and $p53^{-/-}$ mBM-MSCs compared with $p53^{+/+}$ mBM-MSCs; however, no significant differences in the protein expression levels were observed between $p53^{+/-}$ and $p53^{-/-}$ mBM-MSCs (Fig. 5C).

Differential miRNA expression in mBM-MSCs. To establish whether p53 gene exerted its activity through microRNAs (miRNAs), RT-qPCR was performed to determine the levels of miRNAs in mBM-MSCs with differential p53 expression, that have previously been reported to serve vital roles in cancer progression, including miR-221, miR-155, miR-1288, miR-4669, miR-3152 and miR-337 (Fig. 6A) (28-39). The expression levels of miR-3152 and miR-337 were significantly increased in $p53^{+/-}$ and $p53^{-/-}$ mBM-MSCs compared with $p53^{+/+}$ mBM-MSCs, whereas the expression levels of miR-221, miR-155, miR-1288 and miR-4669 were significantly decreased in $p53^{+/-}$ and $p53^{-/-}$ mBM-MSCs compared with $p53^{+/+}$ mBM-MSCs (Fig. 6A). Among these miRNAs, miR-3152, miR-337 and miR-221 were expressed at significantly higher levels in the $p53^{-/-}$ mBM-MSCs compared with $p53^{+/-}$ (Fig. 6A).

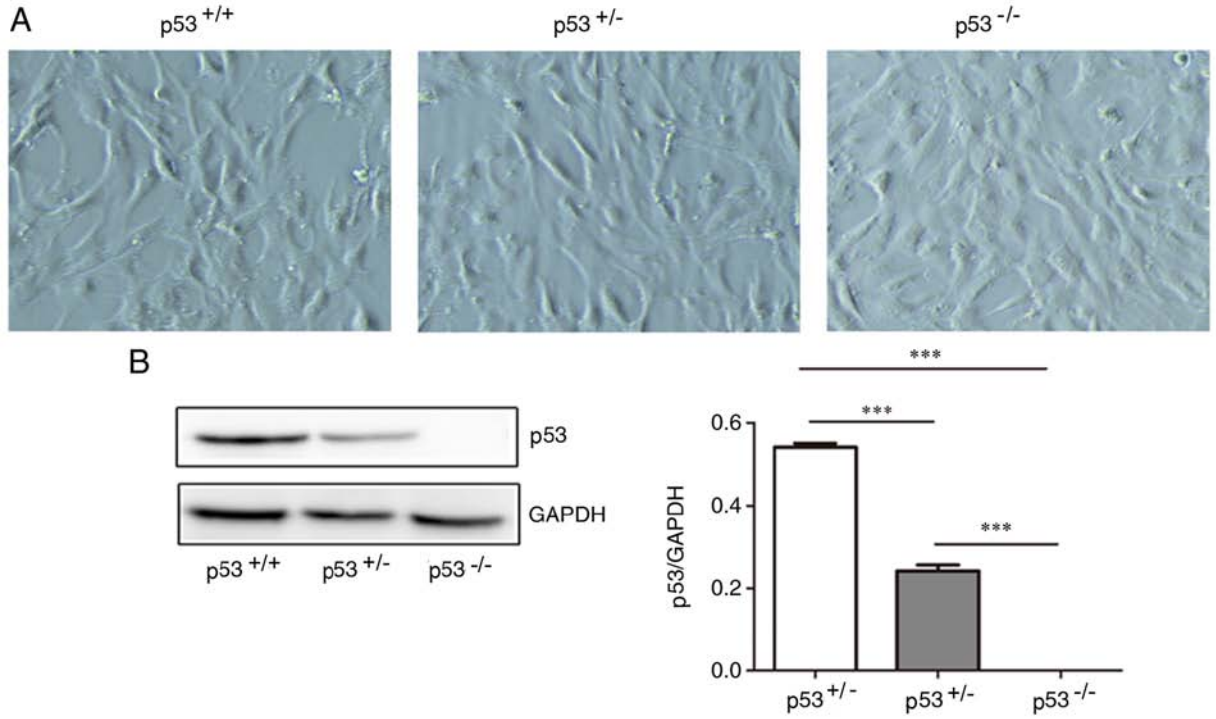

Figure 1. p53 status-related morphology of mBM-MSCs. (A) Representative micrographs of $p53^{+/+}$, $p53^{+/-}$ and $p53^{-/-}$ mBM-MSCs. Magnification, x20. (B) Western blot assay and densitometric analysis of p53 protein expression levels in $p53^{+/+}$, $p53^{+/-}$ and $p53^{-/-}$ mBM-MSCs. ***P<0.001. mBM-MSCs, mouse bone marrow mesenchymal stem cells.

Inflammatory cytokine secretion. To determine whether p53 status affected inflammatory cytokine secretion from mBM-MSCs, the Luminex analysis system was used to determine the content of several inflammation- and cancer-related cytokines in the cell culture supernatant. The expression levels of TNF-α and IP-10 were significantly upregulated in the supernatant of $p53^{+/-}$ and $p53^{-/-}$ mBM-MSCs compared with $p53^{+/+}$ mBM-MSCs (Fig. 6B); however, whilst $p53^{+/-}$ mBM-MSCs secreted significantly less IP-10 compared with $p53^{-/-}$ mBM-MSCs, they secreted higher levels of TNFα compared with $p53^{-/-}$ mBM-MSCs, but no statistical difference was observed (Fig. 6B).

Differential protein expression of mBM-MSCs. Previous proteomic analysis has confirmed that UBR2, RNF31 and MMP19 are enriched in human umbilical cord MSC-derived exosomes (40); the three proteins were reported to promote cellular proliferation and metastasis in tumor progression (41-43). The protein expression levels of the three proteins in $p53^{+/-}$ and $p53^{-/-}$ mBM-MSCs were significantly higher compared with $p53^{+/+}$ mBM-MSCs (Fig. 6C); however, no significant differences in the protein expression levels of the three proteins were observed between $p53^{+/-}$ and $p53^{-/-}$ mBM-MSCs (Fig. 6C).

Discussion

The tumor suppressor gene p53 has numerous functions in biological processes, such as bone homeostasis, organogenesis and neoplasia (24). However, the role of MSCs exhibiting differential p53 statuses remains poorly described. In the present study, p53 wild-type ($p53^{+/+}$), p53 knockdown ($p53^{+/-}$) and p53 knockout ($p53^{-/-}$) mBM-MSCs were analyzed to determine the effect of p53 on the biology of MSCs. Successful isolation, purification and culture of mBM-MSCs revealed that $p53^{+/+}$, $p53^{+/-}$ and $p53^{-/-}$ mBM-MSCs all presented with a fibroblast-like appearance; they all positively expressed the typical surface antigens, CD29, CD44, CD90, and negatively expressed CD34, CD45, and CD11b (44,45). Thus, despite the three groups of mBM-MSCs exhibiting differential p53 levels, no noticeable difference was observed in their morphology and surface antigens presentation.

Previous studies in primary murine cells reported that p53 accumulation and stabilization could promote increased apoptosis and induce cell cycle arrest (46,47). The present study demonstrated, through growth curve assays and DNA cell cycle analysis, that $p53^{+/-}$ and $p53^{-/-}$ mBM-MSCs possessed a higher proliferative potential compared with $p53^{+/+}$ mBM-MSCs, and that the absence, or partial absence, of p53 corresponded with an increased S phase rate within the cell cycle compared with basal p53 levels. These results revealed that the differential expression of p53 influenced the cell cycle distribution and proliferation of MSCs, which is consistent with a previous study (18). The presence and correct functioning of p53 is essential to avoid the spontaneous transformation of MSCs; with the long-term absence of p53 promoting genomic instability in MSCs, and eventually tumorigenesis (23). Results from the present study indicated that the p53 status did not affect tumorigenic ability, and no malignant transformation arising from mBM-MSCs with distinct p53 status was evident over the three-month period *in vivo*, indicating the maintenance of genomic stability of the three mBM-MSC groups across the time period. Extended time-points and cell passages may be required to observe the transformation process *in vivo*.

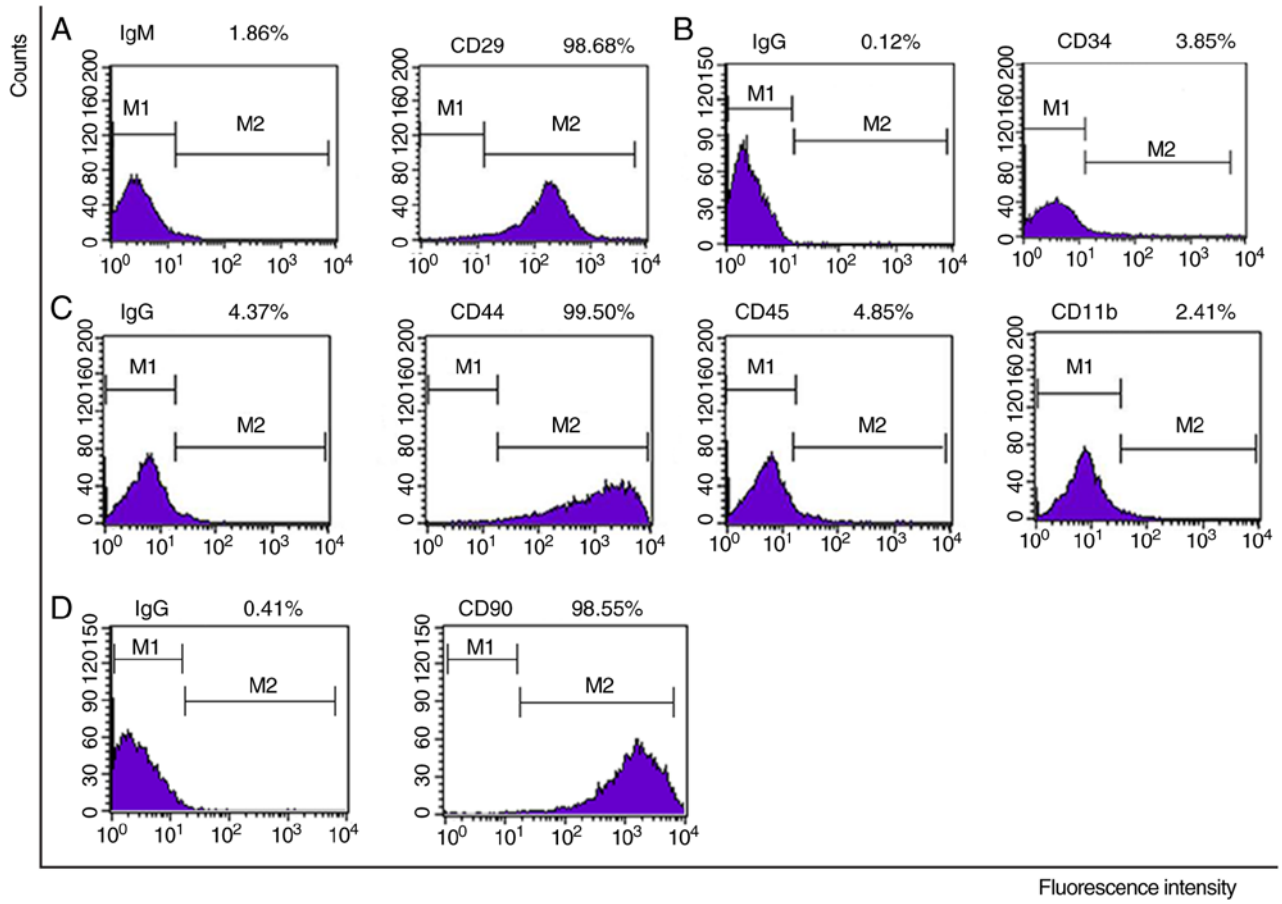

Figure 2. Flow cytometric analysis of cell surface markers on $p53^{+/+}$ mouse bone marrow mesenchymal stem cells. Expression of cell surface markers (A) CD29, (B) CD34, (C) CD44, CD45 and CD11b, and (D) CD90 compared with the IgG or IgM.

MSCs are multipotent and differentiate into diverse cell types; however, the role of p53 in the regulation of this differentiation process is relatively unknown. He *et al* (22) reported that mBM-MSCs deficient in p53 exhibit enhanced osteogenic differentiation properties, but similar adipogenic differentiation properties compared with mBM-MSCs with wild-type p53. Boregowda *et al* (24) demonstrated that the loss of p53 strongly skews MSCs towards an osteogenic fate at the expense of adipogenesis, due to the depletion of mitochondrial ROS, which was induced in a closed low-oxygen (5%) cultured environment. The present study revealed that $p53^{+/-}$ and $p53^{-/-}$ mBM-MSCs have significantly increased adipogenic and osteogenic differentiation ability compared with $p53^{+/+}$ mBM-MSCs, which agrees with a previous study by Armesilla-Diaz *et al* (23). Thus, the differentiation processes of MSCs may be controlled by several factors, including p53, and the discrepancies of its role in adipogenic differentiation will require further investigation.

p53 can inhibit the proliferation and migration of cancer cells. As demonstrated in the current study, a gradual increase in the proliferative and migratory ability was observed during the culture of $p53^{+/-}$ and $p53^{-/-}$ mBM-MSCs compared with $p53^{+/+}$ mBM-MSCs. These results may be partly due to an increased S phase rate and an augmented proliferation rate compared with $p53^{+/+}$ cells. It has been previously reported that the deregulation of p53 pathway components is implicated in cancer cell stemness, invasion, migration and proliferation; for example, the loss of p53 leads to an increased expression of stemness markers, such as Sox2, SALL4 and Oct4, in breast tumors (48). The loss of function of wild-type p53 has also been associated with the promotion of bone metastasis in prostate cancer, partially through the increased expression of stem-like markers in cancer cells (49). Moreover, exosomes from $p53^{-/-}$ mBM-MSC cells demonstrate increased expression of stemness-related genes, such as Oct4, Nanog and Sox2 compared with $p53^{+/+}$ mBM-MSC cells (41). Therefore, the present study investigated these stemness-related proteins to determine the relationship between p53 and stemness. Similar to previous studies (41,46,47), the expression levels of stemness-related proteins, such as LIN28B, Sox2, c-Myc, SALL4 and Oct4 were increased in $p53^{+/-}$ and $p53^{-/-}$ mBM-MSCs, suggesting a positive role of p53 inactivation in stemness maintenance.

Increasing evidence indicates that many miRNAs are closely associated with p53, and p53 has been demonstrated to promote the maturation and expression of miRNAs (50-52), in addition to affecting protein expression and exerting different biological effects through its relevant miRNAs (22,49,53). miRNAs associated with tumor proliferation and metastasis are differentially expressed between gastric cancer (GC) tissue-derived MSCs and adjacent non-cancerous tissue-derived MSCs (54). Moreover, miR-3152 is involved in the therapeutic response to neoadjuvant radio-chemotherapy resistance observed in squamous

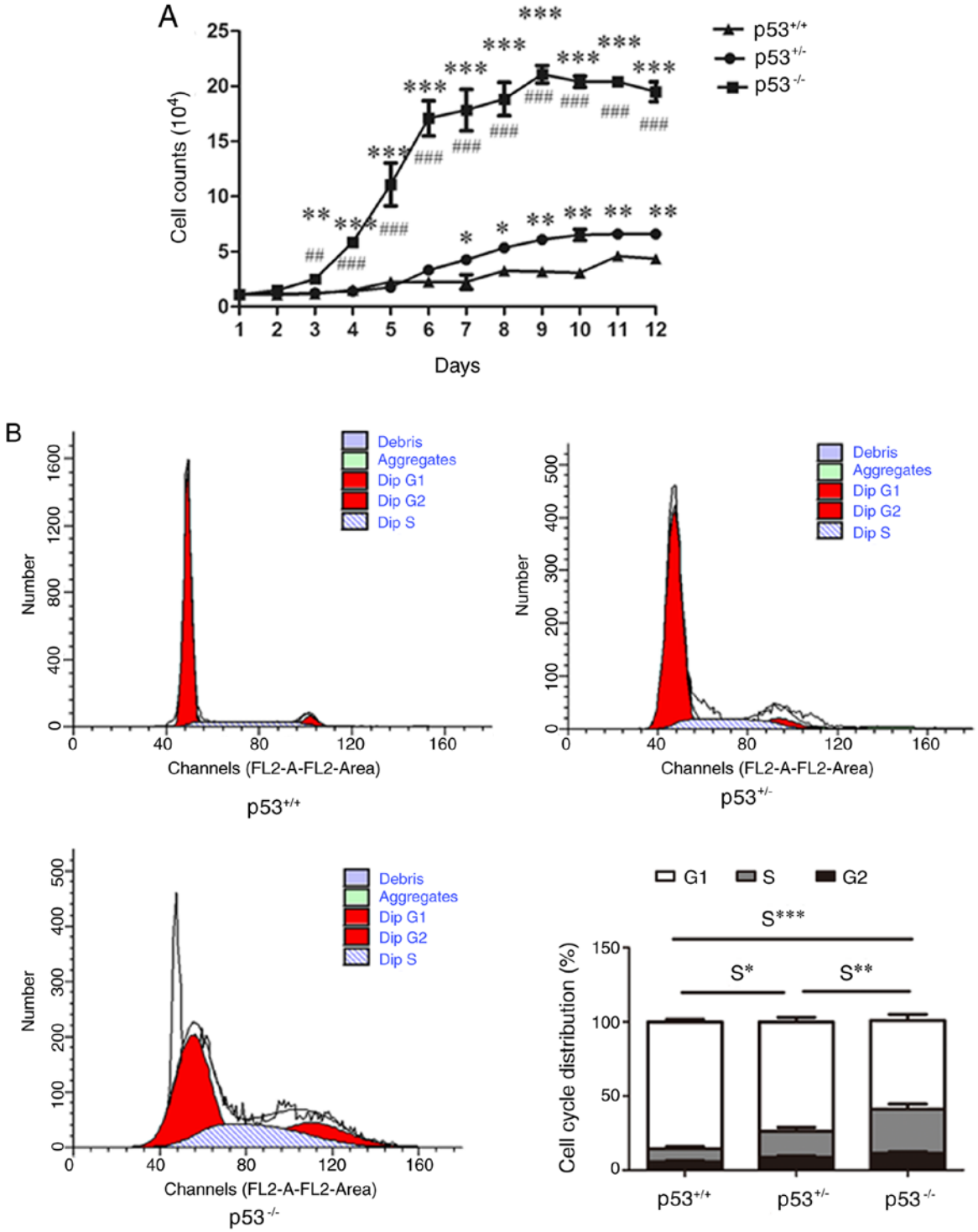

Figure 3. Proliferation and cell cycle analysis of mBM-MSCs with differential p53 statuses. (A) Growth curves of $p53^{+/+}$, $p53^{+/-}$ and $p53^{-/-}$ mBM-MSCs cultured for 12 days, expressed as cell count. *P<0.05, **P<0.01 and ***P<0.001 vs. $p53^{+/+}$ mBM-MSCs; $^{\#\#}$P<0.01 and $^{\#\#\#}$P<0.001 vs. $p53^{+/-}$ mBM-MSCs. (B) Flow cytometric cell cycle analysis of $p53^{+/+}$, $p53^{+/-}$ and $p53^{-/-}$ mBM-MSCs. *P<0.05, **P<0.01 and ***P<0.001. mBM-MSCs, mouse bone marrow mesenchymal stem cells; S, S phase comparison.

cell carcinoma of esophagus (ESCC), which suggested that miR-3152 could act as a predictive biomarker for pre-therapeutic patient selection (28). miR-377 drives malignant characteristics and acts as a prognostic biomarker in multiple different cancers (29-32), whereas miR-221 is involved in osteosarcoma and GC progression (33,34). miR-155 has previously been observed to regulate melanoma cell growth by acting as a tumor suppressor (35), and it is overexpressed in hematological malignancies and solid tumors (36). The differential regulation of miR-1288 was discovered to be related to the cancer location and the pathological staging in colorectal cancers (37). In addition, the overexpression of miR-1288 serves a crucial role in the pathogenesis of ESCC, with its modulation demonstrating potential therapeutic value in patients with ESCC (38). Serum miR-4669 was expressed at lower levels in colon cancer compared to colon controls,

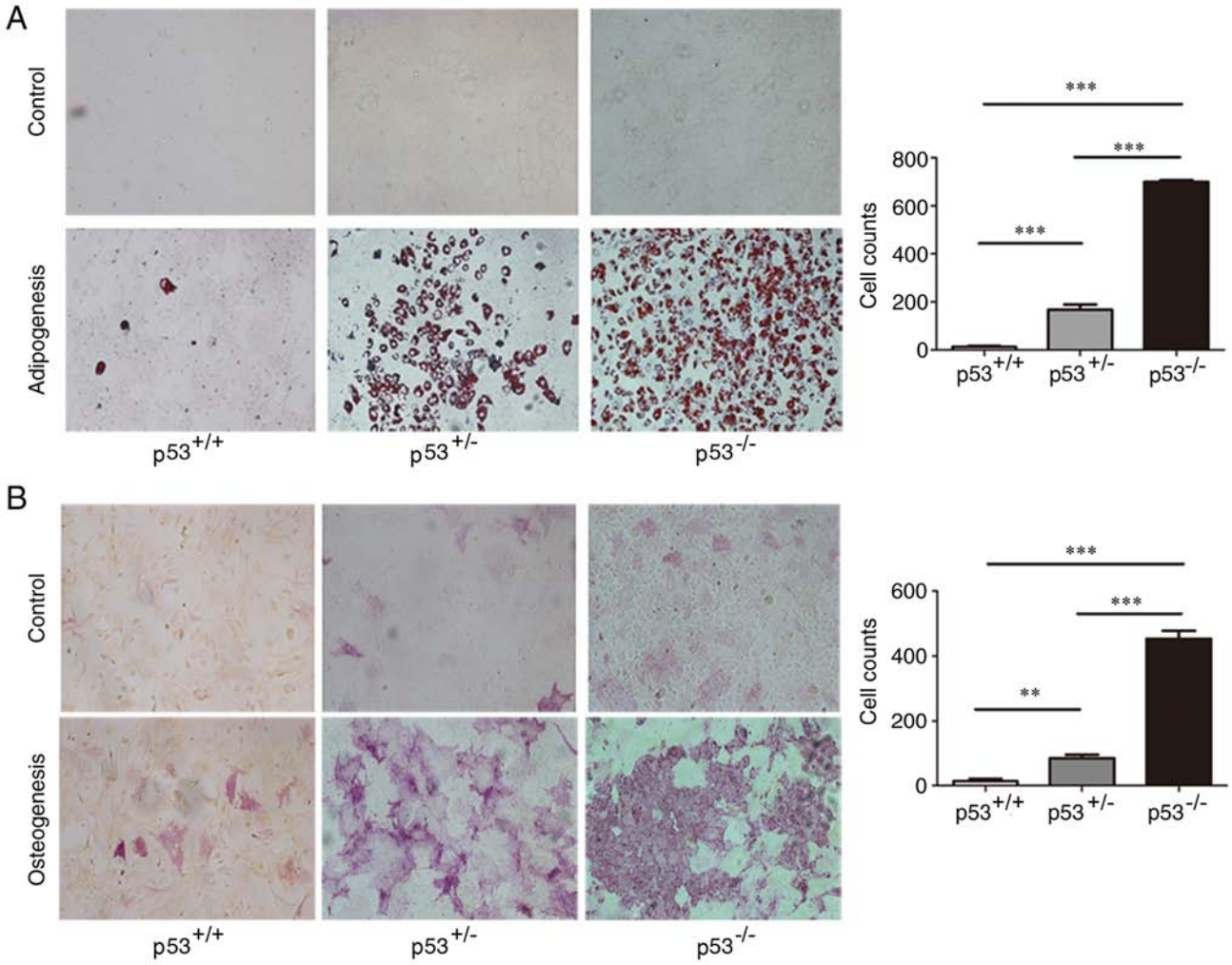

Figure 4. Adipogenic and osteogenic differentiation of mBM-MSCs with differential p53 statuses. (A) $p53^{+/+}$, $p53^{+/-}$ and $p53^{-/-}$ mBM-MSCs were cultured with or without adipogenic induction medium for 14 days and stained with Oil Red O. Magnification, x100. (B) $p53^{+/+}$, $p53^{+/-}$ and $p53^{-/-}$ mBM-MSCs were cultured in osteogenic induction medium for 7 days and subsequently stained with alkaline phosphatase. Magnification, x100. $^{**}P<0.01$ and $^{***}P<0.001$. mBM-MSCs, mouse bone marrow mesenchymal stem cells.

which may facilitate the diagnosis of colon cancer (39). To determine whether the above miRNAs were regulated by p53, the differential expression of these miRNAs in $p53^{+/+}$, $p53^{+/-}$ and $p53^{-/-}$ mBM-MSCs was investigated. The results revealed that miR-3152 and miR-377 were highly expressed in $p53^{+/-}$ and $p53^{-/-}$ mBM-MSCs, which is consistent with their expression levels in other types of cancer (28-32) and suggested that they served an oncogenic role following p53 inactivation. Conversely, miR-221, miR-155 and miR-4669 expression levels were observed to be decreased in $p53^{+/-}$ and $p53^{-/-}$ mBM-MSCs, which based on previous studies (32-39), suggested that they may serve a tumor suppressive role in MSCs. In fact, p53 has been found to serve an important role in cell proliferation and metastasis by acting through cancer-related miRNAs (28-39,53,54).

Data from the present study revealed that the protein levels of UBR2, RNF31 and MMP19 were significantly elevated in $p53^{+/-}$ and $p53^{-/-}$ mBM-MSCs compared with $p53^{+/+}$. Similarly, it was previously reported that UBR2 was highly expressed in $p53^{-/-}$ mBM-MSC cells and exosomes, which served an important role in GC progression (41). RNF31 has been reported to control important oncogenic pathways, such as p53, in breast cancer (42). The increased expression of MMP19 was associated with the progression of cutaneous melanoma and may augment melanoma growth through promoting the invasion of tumor cells (43). Thus, these results suggested a relationship between p53 and UBR2, RNF31 and MMP19 proteins, which were determined to be novel proteins in the p53 signaling pathway and suggested that they may have an oncogenic role in MSCs.

MSCs are known to secrete proteins, including growth factors, inflammatory cytokines and chemokines to regulate their biology in an autocrine or paracrine manner in accordance to the surrounding microenvironment (55). TNF-α is an important factor in the tumor microenvironment; it assists leukemia cells in immune evasion, survival and resistance to chemotherapy (56). The BM microenvironment in patients with multiple myeloma (MM) exhibit elevated concentrations of IP-10, which might not only be a diagnostic tool, but also a predictive biomarker for patients with MM (57). In the present study, it was demonstrated that $p53^{+/-}$ and $p53^{-/-}$ mBM-MSCs secreted higher levels of TNF-α and IP-10, which could subsequently promote their proliferation, according to previous studies (56,57).

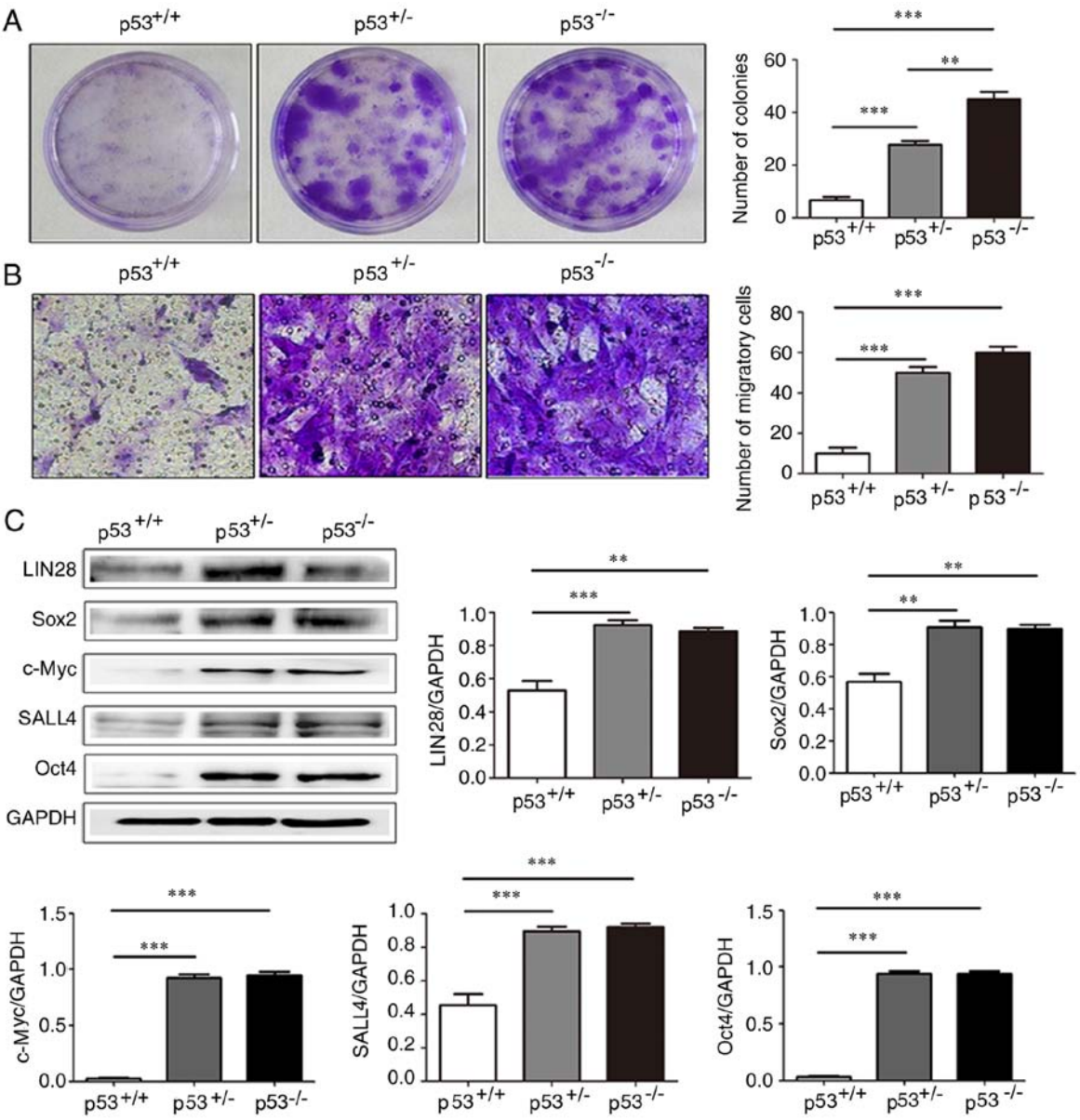

Figure 5. Colony forming and migratory ability, and the expression of stemness-related proteins in, mBM-MSCs with differential levels of p53 expression. (A) Colony formation assay of $p53^{+/+}$, $p53^{+/-}$ and $p53^{-/-}$ mBM-MSCs. (B) Migration assay of $p53^{+/+}$, $p53^{+/-}$ and $p53^{-/-}$ mBM-MSCs. (C) Western blot assay and densitometric analysis for the expression of LIN28B, Sox2, c-Myc, SALL4 and Oct4 in $p53^{+/+}$, $p53^{+/-}$ and $p53^{-/-}$ mBM-MSCs. $^{**}P<0.01$ and $^{***}P<0.001$. LIN28B, protein lin-28 homolog B; mBM-MSCs, mouse bone marrow mesenchymal stem cells; Oct4, octamer binding protein 4; SALL4, Sal-like protein 3.

Compared to $p53^{+/+}$ MSCs, which expressed the highest levels of p53 protein, the *in vitro* $p53^{+/-}$ MSCs, rather than the complete absence of p53 ($p53^{-/-}$ MSCs), were sufficient to induce changes in the biological functions observed in this study, such as cell proliferation, migration, differentiation and the cell cycle. Compared with $p53^{+/-}$ cells demonstrating an intermediate level of p53 expression, $p53^{-/-}$ cells presented inconsistent differences in the different biological functions investigated. These observations suggested that distinct thresholds of p53 protein expression levels were responsible for its various functions during the progression from p53 knockdown to inactivation. It is therefore necessary to determine whether additional mechanisms are contributing as well to drive these biological characteristics.

In conclusion, the present study compared the differential characteristics of $p53^{+/+}$, $p53^{+/-}$ and $p53^{-/-}$ mBM-MSCs, and discovered that they exhibited and shared typical MSC characteristics, but also had some differences, such as the rate of proliferation, differentiation, colony formation, migration and the expression of stemness-related proteins, tumor-associated miRNAs and proteins, as well as inflammatory cytokines. The partial or total absence of p53 may positively regulate the biological function of MSCs through its relevant miRNAs and proteins. Moreover, the autocrine or paracrine secretion of growth factors, inflammatory cytokines and chemokines may provide the mechanism by which MSCs perform these roles. However, the present study only briefly investigated the functions of different p53 statuses in cells, and the relationship between p53 and the molecules found to be differentially expressed was only inferred; future studies are required to investigate the casual relationship and the regulation between p53 and these molecules. In addition, further research is

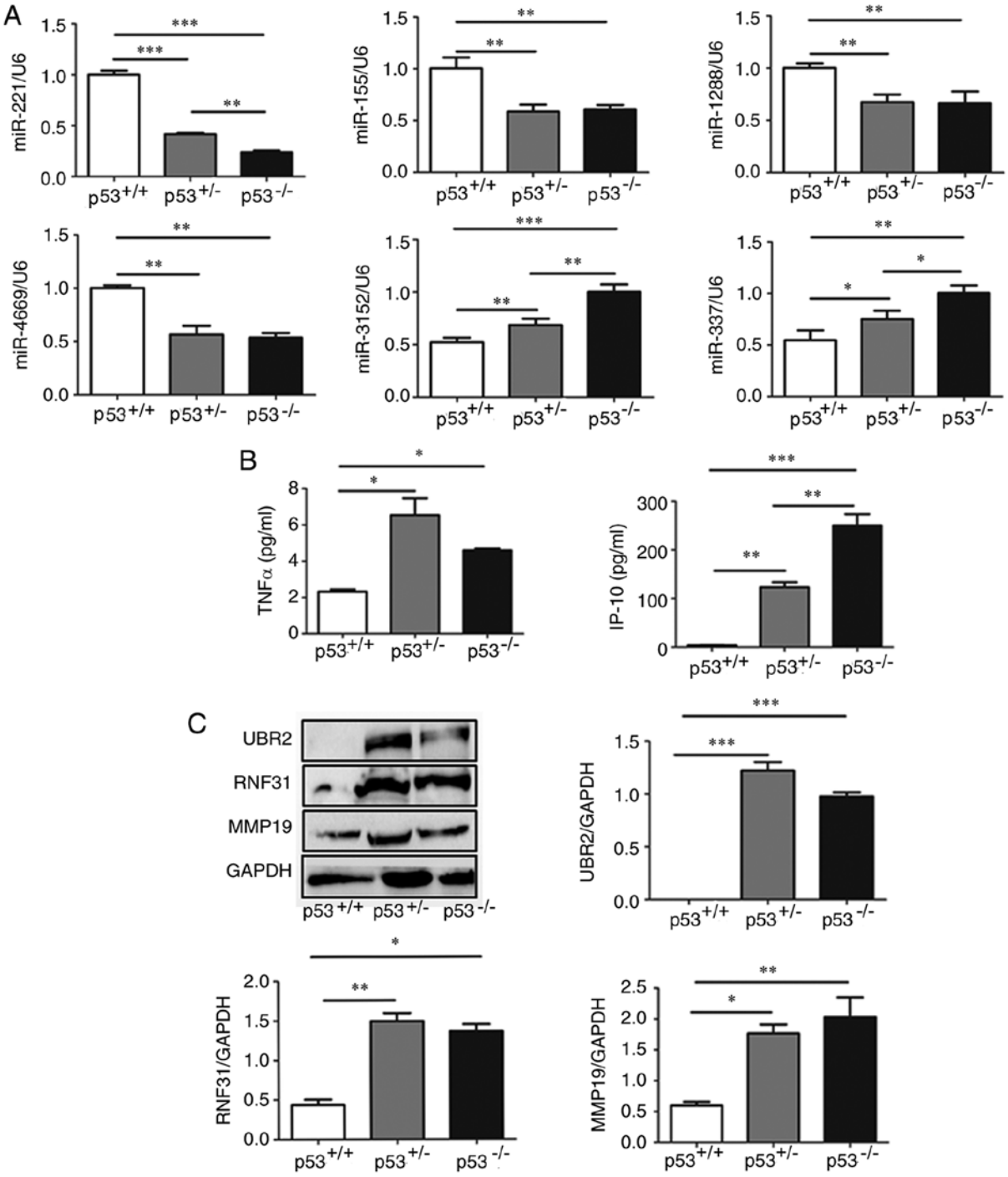

Figure 6. Expression of miRNAs, cytokines and proteins in mBM-MSCs with differential p53 statuses. (A) Reverse transcription-quantitative PCR analysis of miRNAs expression levels of in $p53^{+/+}$, $p53^{+/-}$ and $p53^{-/-}$ mBM-MSCs; expressions were normalized to U6. (B) Luminex assay of TNFα and IP-10 secretion in the supernatant obtained from $p53^{+/+}$, $p53^{+/-}$ and $p53^{-/-}$ mBM-MSCs. (C) Western blotting and densitometric analysis of protein expression levels of UBR2, RNF31 and MMP19 in $p53^{+/+}$, $p53^{+/-}$ and $p53^{-/-}$ mBM-MSCs; GAPDH was used as a loading control. *P<0.05, **P<0.01 and ***P<0.001. IP-10, interferon-γ-inducible protein; mBM-MSCs, mouse bone marrow mesenchymal stem cells; miR/miRNA, microRNA; MMP19, matrix metalloproteinase 19; RNF31, RING-finger protein 31; TNFα, tumor necrosis factor α; UBR2, ubiquitin protein ligase E3 component n-recognin.

required to investigate how p53 regulates the function of MSCs through these genes and proteins. Overall, this study may provide new evidence for the biological regulatory role of p53 in BM-MSCs.

Acknowledgements

Not applicable.

Funding

This study was supported by The National Natural Science Foundation of China (grant no. 81702078), The Natural Science Foundation of Jiangsu Province (grant no. BK20170356), The Natural Science Fund for Colleges and Universities of Jiangsu Province (grant no. 17KJB320016), The Suzhou Science and Technology Project (grant no. SYS201728), The Postgraduate

Research & Practice Innovation Program of Jiangsu Province (grant no. KYCX18_2535) and The Young Stuff Pre-research Fund Project of The Second Affiliated Hospital of Soochow University (grant no. SDFEYQN1718).

Availability of data and materials

All data generated or analyzed during this study are included in this published article.

Authors' contributions

HY and HD conceived and designed the experiments. BW, LW, JM, HW, LX and YR performed the experiments. HY analyzed the data and wrote the manuscript. All authors read, reviewed and approved the final manuscript.

Ethics approval and consent to participate

All experimental procedures involving animals were in accordance with the Guide for the Care and Use of Laboratory Animals and approved by the Animal Use Ethics Committee of Jiangsu University (Zhejiang, China; 2012258).

Patient consent for publication

Not applicable.

Competing interests

The authors declare that they have no competing interests.

References

1. Frausin S, Viventi S, Verga Falzacappa L, Quattromani MJ, Leanza G, Tommasini A and Valencic E: Wharton's jelly derived mesenchymal stromal cells: Biological properties, induction of neuronal phenotype and current applications in neurodegeneration research. Acta Histochem 117: 329-338, 2015.
2. Iser IC, Bracco PA, Gonçalves CE, Zanin RF, Nardi NB, Lenz G, Battastini AM and Wink MR: Mesenchymal stem cells from different murine tissues have differential capacity to metabolize extracellular nucleotides. J Cell Biochem 115: 1673-1682, 2014.
3. Jung J, Choi JH, Lee Y, Park JW, Oh IH, Hwang SG, Kim KS and Kim GJ: Human placenta-derived mesenchymal stem cells promote hepatic regeneration in CCl4-injured rat liver model via increased autophagic mechanism. Stem Cells 31: 1584-1596, 2013.
4. Pittenger MF, Mackay AM, Beck SC, Jaiswal RK, Douglas R, Mosca JD, Moorman MA, Simonetti DW, Craig S and Marshak DR: Multilineage potential of adult human mesenchymal stem cells. Science 284: 143-147, 1999.
5. Sargent A and Miller RH: MSC therapeutics in chronic inflammation. Curr Stem Cell Rep 2: 168-173, 2016.
6. Huang F, Wang M, Yang T, Cai J, Zhang Q, Sun Z, Wu X, Zhang X, Zhu W, Qian H and Xu W: Gastric cancer-derived MSC-secreted PDGF-DD promotes gastric cancer progression. J Cancer Res Clin Oncol 140: 1835-1848, 2014.
7. Homma A, Nakamura K, Matsuura K, Mizusawa J, Onimaru R, Fukuda H and Fujii M: Dose-finding and efficacy confirmation trial of superselective intra-arterial infusion of cisplatin and concomitant radiotherapy for patients with locally advanced maxillary sinus cancer (JCOG1212, RADPLAT-MSC). Jpn J Clin Oncol 45: 119-122, 2015.
8. Cuiffo BG, Campagne A, Bell GW, Lembo A, Orso F, Lien EC, Bhasin MK, Raimo M, Hanson SE, Marusyk A, *et al*: MSC-regulated microRNAs converge on the transcription factor FOXP2 and promote breast cancer metastasis. Cell Stem Cell 15: 762-774, 2014.
9. da Costa Gonçalves F, Grings M, Nunes NS, Pinto FO, Garcez TN, Visioli F, Leipnitz G and Paz AH: Antioxidant properties of mesenchymal stem cells against oxidative stress in a murine model of colitis. Biotechnol Lett 39: 613-622, 2017.
10. Ansboro S, Roelofs AJ and De Bari C: Mesenchymal stem cells for the management of rheumatoid arthritis: Immune modulation, repair or both? Curr Opin Rheumatol 29: 201-207, 2017.
11. Nair BC, Krishnan SR, Sareddy GR, Mann M, Xu B, Natarajan M, Hasty P, Brann D, Tekmal RR and Vadlamudi RK: Proline, glutamic acid and leucine-rich protein-1 is essential for optimal p53-mediated DNA damage response. Cell Death Differ 21: 1409-1418, 2014.
12. Shi Y, Du L, Lin L and Wang Y: Tumour-associated mesenchymal stem/stromal cells: Emerging therapeutic targets. Nat Rev Drug Discov 16: 35-52, 2017.
13. Tu B, Zhu J, Liu S, Wang L, Fan Q, Hao Y, Fan C and Tang TT: Mesenchymal stem cells promote osteosarcoma cell survival and drug resistance through activation of STAT3. Oncotarget 7: 48296-48308, 2016.
14. Zhu M, Wang M, Yang F, Tian Y, Cai J, Yang H, Fu H, Mao F, Zhu W, Qian H and Xu W: miR-155-5p inhibition promotes the transition of bone marrow mesenchymal stem cells to gastric cancer tissue derived MSC-like cells via NF-κB p65 activation. Oncotarget 7: 16567-16580, 2016.
15. O'Malley G, Heijltjes M, Houston AM, Rani S, Ritter T, Egan LJ and Ryan AE: Mesenchymal stromal cells (MSCs) and colorectal cancer: A troublesome twosome for the anti-tumour immune response? Oncotarget 7: 60752-60774, 2016.
16. Zhang M, Gao CE, Li WH, Yang Y, Chang L, Dong J, Ren YX and Chen D: Microarray based analysis of gene regulation by mesenchymal stem cells in breast cancer. Oncol Lett 13: 2770-2776, 2017.
17. Li N, Xie C and Lu NH: p53, a potential predictor of Helicobacter pylori infection-associated gastric carcinogenesis? Oncotarget 7: 66276-66286, 2016.
18. Berkers CR, Maddocks OD, Cheung EC, Mor I and Vousden KH: Metabolic regulation by p53 family members. Cell Metab 18: 617-633, 2013.
19. Quintas-Cardama A, Hu C, Qutub A, Qiu YH, Zhang X, Post SM, Zhang N, Coombes K and Kornblau SM: p53 pathway dysfunction is highly prevalent in acute myeloid leukemia independent of TP53 mutational status. Leukemia 31: 1296-1305, 2017.
20. Wang XJ, L Jeffrey Medeiros, Bueso-Ramos CE, Tang G, Wang S, Oki Y, Desai P, Khoury JD, Miranda RN, Tang Z, *et al*: P53 expression correlates with poorer survival and augments the negative prognostic effect of MYC rearrangement, expression or concurrent MYC/BCL2 expression in diffuse large B-cell lymphoma. Mod Pathol 30: 194-203, 2017.
21. Tataria M, Quarto N, Longaker MT and Sylvester KG: Absence of the p53 tumor suppressor gene promotes osteogenesis in mesenchymal stem cells. J Pediatr Surg 41: 624-632, 2006.
22. He Y, de Castro LF, Shin MH, Dubois W, Yang HH, Jiang S, Mishra PJ, Ren L, Gou H, Lal A, *et al*: p53 loss increases the osteogenic differentiation of bone marrow stromal cells. Stem Cells 33: 1304-1319, 2015.
23. Armesilla-Diaz A, Elvira G and Silva A: p53 regulates the proliferation, differentiation and spontaneous transformation of mesenchymal stem cells. Exp Cell Res 315: 3598-3610, 2009.
24. Boregowda SV, Krishnappa V, Strivelli J, Haga CL, Booker CN and Phinney DG: Basal p53 expression is indispensable for mesenchymal stem cell integrity. Cell Death Differ 25: 677-690, 2018.
25. Huang Y, Yu P, Li W, Ren G, Roberts AI, Cao W, Zhang X, Su J, Chen X, Chen Q, *et al*: p53 regulates mesenchymal stem cell-mediated tumor suppression in a tumor microenvironment through immune modulation. Oncogene 33: 3830-3838, 2014.
26. Patocs A, Zhang L, Xu Y, Weber F, Caldes T, Mutter GL, Platzer P and Eng C: Breast-cancer stromal cells with TP53 mutations and nodal metastases. N Engl J Med 357: 2543-2551, 2007.
27. Livak JK and Schmittgen TD: Analysis of relative gene expression data using quantitative PCR and the 2(-Delta Delta C(T)) method. Methods 25: 402-408, 2001.
28. Slotta-Huspenina J, Drecoll E, Feith M, Habermehl D, Combs S, Weichert W, Bettstetter M, Becker K and Langer R: MicroRNA expression profiling for the prediction of resistance to neoadjuvant radiochemotherapy in squamous cell carcinoma of the esophagus. J Transl Med 16: 109, 2018.
29. Wu H, Liu HY, Liu WJ, Shi YL and Bao D: miR-377-5p inhibits lung cancer cell proliferation, invasion, and cell cycle progression by targeting AKT1 signaling. J Cell Biochem: Nov 28, 2018: doi: 10.1002/jcb.28091 (Epub ahead of print).

30. Wang CQ, Chen L, Dong CL, Song Y, Shen ZP, Shen WM and Wu XD: MiR-377 suppresses cell proliferation and metastasis in gastric cancer via repressing the expression of VEGFA. Eur Rev Med Pharmacol Sci 21: 5101-5111, 2017.
31. El Baroudi M, Machiels JP and Schmitz S: Expression of SESN1, UHRF1BP1, and miR-377-3p as prognostic markers in mutated TP53 squamous cell carcinoma of the head and neck. Cancer Biol Ther 18: 775-782, 2017.
32. Liu WY, Yang Z, Sun Q, Yang X, Hu Y, Xie H, Gao HJ, Guo LM, Yi JY, Liu M and Tang H: miR-377-3p drives malignancy characteristics via upregulating GSK-3β expression and activating NF-κB pathway in hCRC cells. J Cell Biochem 119: 2124-2134, 2018.
33. Hu XH, Zhao ZX, Dai J, Geng DC and Xu YZ: MicroRNA-221 regulates osteosarcoma cell proliferation, apoptosis, migration, and invasion by targeting CDKN1B/p27. J Cell Biochem 120: 4665-4674, 2019.
34. Feng Y, Bai F, You Y, Bai F, Wu C, Xin R, Li X and Nie Y: Dysregulated microRNA expression profiles in gastric cancer cells with high peritoneal metastatic potential. Exp Ther Med 16: 4602-4608, 2018.
35. DiSano JA, Huffnagle I, Gowda R, Spiegelman VS, Robertson GP and Pameijer CR: Loss of miR-155 upregulates WEE1 in metastatic melanoma. Melanoma Res 29: 216-219, 2019.
36. Witten LW, Cheng CJ and Slack FJ: miR-155 drives oncogenesis by promoting and cooperating with mutations in the c-Kit oncogene. Oncogene 38: 2151-2161, 2019.
37. Gopalan V, Pillai S, Ebrahimi F, Salajegheh A, Lam TC, Le TK, Langsford N, Ho YH, Smith RA and Lam AK: Regulation of microRNA-1288 in colorectal cancer: Altered expression and its clinicopathological significance. Mol Carcinog 53 (Suppl 1): E36-E44, 2014.
38. Gopalan V, Islam F, Pillai S, Tang JC, Tong DK, Law S, Chan KW and Lam AK: Overexpression of microRNA-1288 in oesophageal squamous cell carcinoma. Exp Cell Res 348: 146-154, 2016.
39. Wang YN, Chen ZH and Chen WC: Novel circulating microRNAs expression profile in colon cancer: A pilot study. Eur J Med Res 22: 51, 2017.
40. Zhang B, Shi Y, Gong A, Pan Z, Shi H, Yang H, Fu H, Yan Y, Zhang X, Wang M, *et al*: HucMSC Exosome-delivered 14-3-3ζ orchestrates self-control of the Wnt response via modulation of YAP during cutaneous regeneration. Stem Cells 34: 2485-2500, 2016.
41. Mao J, Liang Z, Zhang B, Yang H, Li X, Fu H, Zhang X, Yan Y, Xu W and Qian H: UBR2 Enriched in p53 deficient mouse bone marrow mesenchymal stem Cell-Exosome promoted gastric cancer progression via Wnt/β-catenin pathway. Stem Cells 35: 2267-2279, 2017.
42. Zhu J, Zhuang T, Yang H, Li X, Liu H and Wang H: Atypical ubiquitin ligase RNF31: The nuclear factor modulator in breast cancer progression. BMC Cancer 16: 538, 2016.
43. Müller M, Beck IM, Gadesmann J, Karschuk N, Paschen A, Proksch E, Djonov V, Reiss K and Sedlacek R: MMP19 is upregulated during melanoma progression and increases invasion of melanoma cells. Mod Pathol 23: 511-521, 2010.
44. Sineh Sepehr K, Razavi A, Saeidi M, Mossahebi-Mohammadi M, Abdollahpour-Alitappeh M and Hashemi SM: Development of a novel explant culture method for the isolation of mesenchymal stem cells from human breast tumor. J Immunoassay Immunochem 39: 207-217, 2018.
45. Kang R, Zhou Y, Tan S, Zhou G, Aagaard L, Xie L, Bünger C, Bolund L and Luo Y: Mesenchymal stem cells derived from human induced pluripotent stem cells retain adequate osteogenicity and chondrogenicity but less adipogenicity. Stem Cell Res Ther 6: 144, 2015.
46. Li XF, Xu BZ and Wang SZ: Aspirin inhibits the proliferation and migration of gastric cancer cells in p53-knockout mice. Oncol Lett 12: 3183-3186, 2016.
47. Donehower LA and Lozano G: 20 years studying p53 functions in genetically engineered mice. Nat Rev Cancer 9: 831-841, 2009.
48. Zhang Y, Dube C, Gibert M Jr, Cruickshanks N, Wang B, Coughlan M, Yang Y, Setiady I, Deveau C, Saoud K, *et al*: The p53 pathway in Glioblastoma. Cancers (Basel) 10: pii: E297, 2018.
49. Ren D, Wang M, Guo W, Zhao X, Tu X, Huang S, Zou X and Peng X: Wild-type p53 suppresses the epithelial-mesenchymal transition and stemness in PC-3 prostate cancer cells by modulating miR-145. Int J Oncol 42: 1473-1481, 2013.
50. Tarasov V, Jung P, Verdoodt B, Lodygin D, Epanchintsev A, Menssen A, Meister G and Hermeking H: Differential regulation of microRNAs by p53 revealed by massively parallel sequencing: MiR-34a is a p53 target that induces apoptosis and G1-arrest. Cell Cycle 6: 1586-1593, 2007.
51. Cortez MA, Ivan C, Valdecanas D, Wang X, Peltier HJ, Ye Y, Araujo L, Carbone DP, Shilo K, Giri DK, *et al*: PDL1 Regulation by p53 via miR-34. J Natl Cancer Inst 108: pii: djv303, 2015.
52. Sachdeva M, Zhu S, Wu F, Wu H, Walia V, Kumar S, Elble R, Watabe K and Mo YY: p53 represses c-Myc through induction of the tumor suppressor miR-145. Proc Natl Acad Sci USA 106: 3207-3212, 2009.
53. Chang CJ, Chao CH, Xia W, Yang JY, Xiong Y, Li CW, Yu WH, Rehman SK, Hsu JL, Lee HH, *et al*: p53 regulates epithelial-mesenchymal transition and stem cell properties through modulating miRNAs. Nat Cell Biol 13: 317-323.
54. Wang M, Zhao C, Shi H, Zhang B, Zhang L, Zhang X, Wang S, Wu X, Yang T, Huang F, *et al*: Deregulated microRNAs in gastric cancer tissue-derived mesenchymal stem cells: Novel biomarkers and a mechanism for gastric cancer. Br J Cancer 110: 1199-1210, 2014.
55. Chan JK and Lam PY: Human mesenchymal stem cells and their paracrine factors for the treatment of brain tumors. Cancer Gene Ther 20: 539-543, 2013.
56. Zhou X, Li Z and Zhou J: Tumor necrosis factor α in the onset and progression of leukemia. Exp Hematol 45: 17-26, 2017.
57. Cao Y, Luetkens T, Kobold S, Hildebrandt Y, Gordic M, Lajmi N, Meyer S, Bartels K, Zander AR, Bokemeyer C, *et al*: The cytokine/chemokine pattern in the bone marrow environment of multiple myeloma patients. Exp Hematol 38: 860-867, 2010.